Magnetic phase diagram of La$_{2-x}$Sr$_x$CoO$_4$ revised using muon-spin relaxation

R. C. Williams,[1] F. Xiao,[1] T. Lancaster,[1] R. De Renzi,[2] G. Allodi,[2] S. Bordignon,[2] P. G. Freeman,[3,4,*] F. L. Pratt,[5] S. R. Giblin,[6] J. S. Möller,[7,†] S. J. Blundell,[7] A. T. Boothroyd,[7] and D. Prabhakaran[7]

[1]*Centre for Materials Physics, Durham University, Durham, DH1 3LE, United Kingdom*
[2]*Dipartimento di Fisica e Scienze della Terra, Università degli Studi di Parma, Viale delle Scienze 7A, I-43124 Parma, Italy*
[3]*École Polytechnique Fédérale de Lausanne, ICMP, Lab Quantum Magnetism, CH-1015 Lausanne, Switzerland*
[4]*Institut Laue-Langevin, 71 avenue des Martyrs 38000 Grenoble, France*
[5]*ISIS Facility, STFC Rutherford Appleton Laboratory, Chilton, Didcot, Oxfordshire OX11 0QX, United Kingdom*
[6]*School of Physics and Astronomy, Cardiff University, Queen's Buildings, The Parade, Cardiff CF24 3AA, United Kingdom*
[7]*Oxford University Department of Physics, Clarendon Laboratory, Parks Road, Oxford OX1 3PU, United Kingdom*

We report the results of a muon-spin relaxation (μSR) investigation of La$_{2-x}$Sr$_x$CoO$_4$, an antiferromagnetic insulating series which has been shown to support charge ordered and magnetic stripe phases and an hourglass magnetic excitation spectrum. We present a revised magnetic phase diagram, which shows that the suppression of the magnetic ordering temperature is highly sensitive to small concentrations of holes. Distinct behavior within an intermediate x range ($0.2 \leqslant x \lesssim 0.6$) suggests that the putative stripe ordered phase extends to lower x than previously thought. Further charge doping ($0.67 \leqslant x \leqslant 0.9$) prevents magnetic ordering for $T \gtrsim 1.5$ K.

Thirty years after the discovery of high-T_c superconductivity, the role of multiple order parameters in the cuprates continues to be a topic of intense research, with the interplay between correlations of charge order (CO), antiferromagnetic spin order (SO), and superconductivity the topic of much investigation [1–5]. Although a detailed comparison of specific systems has been found to be problematical, in order to elucidate the details of the physics at play in a different context it is illuminating to study isostructural nonsuperconducting $3d$ transition metal oxides [6] such as the antiferromagnetic series La$_{2-x}$Sr$_x$CoO$_4$ (LSCO). Controlled doping of holes into the two-dimensional CoO$_2$ layers is achieved via substitution of Sr for La but, in contrast to the cuprates, a spin-blockade mechanism means the series remains an insulator for $x \leqslant 1$ [7]. The previously reported phase diagram of LSCO, determined by neutron scattering [8], shows a region of nearest-neighbor antiferromagnetism (nnAFM) for low dopant concentrations ($x \lesssim 0.3$) and incommensurate (IC) magnetism consistent with stripelike CO and SOs for an intermediate doping range $0.3 \lesssim x \lesssim 0.6$. Recently, muon-spin rotation (μSR) and NMR measurements made on the stripe ordered $x = 1/3$ compound [9] revealed the importance of a range of time scales in the magnetic ordering of the material, with μSR showing both the onset of static magnetic order and the freezing of dynamical processes at temperatures significantly lower than the ordering temperature previously identified using neutrons. This is because μSR is sensitive to fluctuations on the microsecond time scale (set by the muon gyromagnetic ratio $\gamma_\mu = 2\pi \times 135.5$ MHz T^{-1}). Such slow fluctuations appear static in neutron scattering measurements where the energy resolution $\Delta E \approx 1$ meV constrains the sensitivity of the technique to fluctuations with a much faster time scale

$\hbar/\Delta E \approx 10^{-11}$ s. This has motivated the μSR investigation of the full phase diagram of the LSCO system reported here, allowing us to probe the influence of slow fluctuations on the low-temperature magnetism across this series and determine a revised phase diagram.

Crystals of LSCO were grown using the floating-zone method, with varying sintering conditions depending on the Sr content x [10]. Such crystals have a tendency for excess oxygen when $x \lesssim 0.3$, similar to the La$_{2-x}$Sr$_x$NiO$_{4+\delta}$ system [11–14]. On this basis we expect that the lowest doped samples have $\delta > 0$, but approach oxygen stoichiometry by $x \approx 0.3$. In a μSR experiment [10,15], spin-polarized positive muons are implanted into the sample and subsequently decay into a positron, emitted preferentially in the direction of the muon's instantaneous spin. Time-dependent asymmetry $A(t)$ is proportional to the muon ensemble's spin polarization. Zero-field measurements were made using the EMU spectrometer at ISIS, and the GPS and DOLLY instruments at the Swiss Muon Source (SμS), with the initial muon polarization directed along the c axis of each crystallite, perpendicular to the planes containing the CoO$_2$ layers.

In data measured at SμS damped oscillations are visible at low temperature in the asymmetry spectra for all concentrations with $x \leqslant 0.5$ [Fig. 1(c), inset]. These are indicative of quasistatic local magnetic fields at the muon sites and confirm the presence of SO. The two precession frequencies observed in most samples indicate two distinct classes of muon site with local field strengths in the approximate ratio 2:1 (for certain concentrations only one frequency is resolvable). There is little doping dependence in the magnitude of the two frequencies, supporting the claim that Co^{3+} ions remain in the low-spin $S = 0$ state throughout this doping range [16–18], and that there is little variation in the moment size of the $S = 3/2$ Co^{2+} ions.

Before considering detailed analysis, we provide a broad survey of the concentration-temperature (x,T) phase diagram that forms the main result of this Rapid Communication. To do this, it is illustrative to consider the average early-time

---

*Present address: Jeremiah Horrocks Institute, University of Central Lancashire, Preston PR1 2HE, United Kingdom.

†Present address: Neutron Scattering and Magnetism, Laboratory for Solid State Physics, ETH Zürich, CH-8093 Zürich, Switzerland.
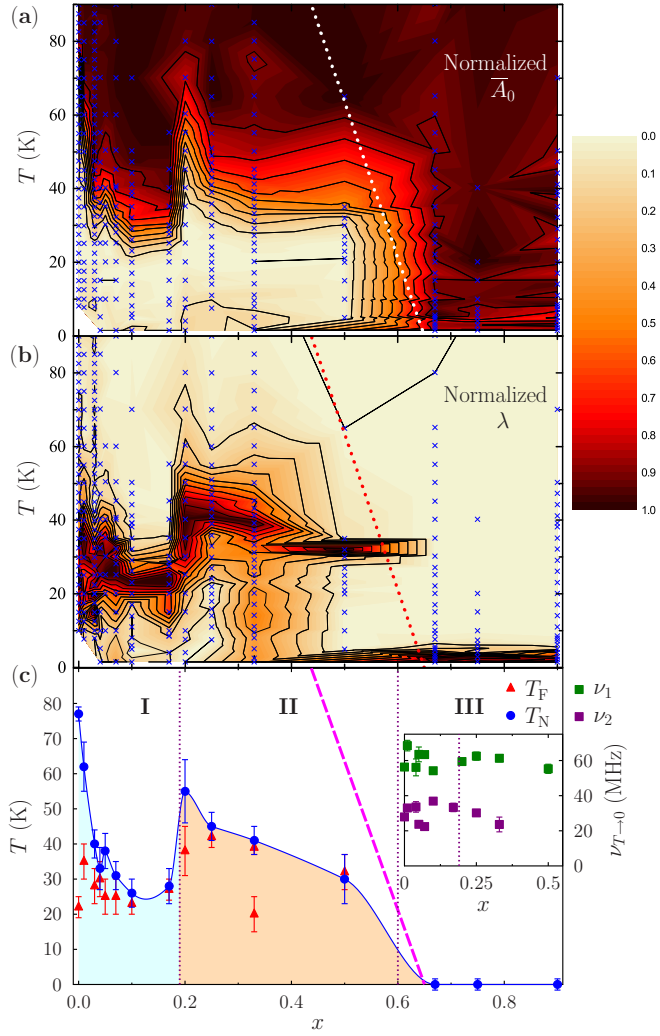
FIG. 1. (a) Normalized early-time initial asymmetry $\overline{A}_0$ in the (x,T) plane. (b) Normalized relaxation rate λ. Crosses identify measured points and the dashed line shows the phase boundary from Ref. [8]. (c) Revised phase diagram showing the nominal transition temperature T_N and freezing temperature T_F. Inset: muon precession frequencies.

asymmetry $\overline{A}_0 \equiv \langle A(t \leqslant 0.13\,\mu s)\rangle$, where the time averaging allows us to identify the depolarization of the muon ensemble due to static or slowly fluctuating magnetism (Fig. 1(a), normalized between extreme values for each asymmetry spectrum [19]). At temperatures well above T_N, the muon spins are insensitive to rapidly fluctuating Co^{2+} moments (motional narrowing), leading to large values of $\overline{A}_0$. For $x \leqslant 0.5$ initial asymmetry is lost upon cooling, reflecting the presence of large internal magnetic fields, such as those giving rise to the oscillations described above. This drop in $\overline{A}_0$ may be fitted [20] with a Fermi-like broadened step function $\overline{A}_0(T) = A_H + (A_L - A_H)/(e^{(T-T_c)/w} + 1)$, which provides a transition temperature T_c by parametrizing the continuous step of width w from high- (A_H) to low-T (A_L) asymmetry [21]. An onset temperature for magnetic ordering may be obtained using $T_N = (T_c + w) \pm w$, and these values are shown in the revised phase diagram, Fig. 1(c). The previous μSR study on

$x = 0.33$ demonstrated sensitivity to slow fluctuations and the freezing of dynamics [9]. To follow these features datasets were heavily binned to filter out high-frequency components and fitted to $A(t) = A_{rel}e^{-(\lambda t)^\beta} + A_b$, where A_{rel} and A_b are the relaxing and nonrelaxing baseline amplitudes, respectively, and β was constrained to be greater than 0.5 [10]. The resulting relaxation rates λ (also normalized) are shown in Fig. 1(b). It is expected that the relaxation rate $\lambda \propto \langle (B - \langle B \rangle)^2 \rangle \tau$ (i.e., the second moment of the magnetic field distribution multiplied by the correlation time τ [22]) reflecting both field distribution widths and fluctuation rates. A peak in λ is often indicative of a freezing of dynamics on the muon time scale as correlation times diverge, and so nominal freezing temperatures T_F (defined as the temperature corresponding to peak values of λ) feature on the phase diagram [Fig. 1(c)].

We distinguish three distinct regions in the phase diagram. For $x < 0.2$ (Region I) the introduction of $S = 0$ Co^{3+} ions suppresses T_N of nnAFM order, and there is evidence for freezing of dynamics at lower temperatures for compounds with small x. For intermediate doping ($0.2 \leqslant x \lesssim 0.6$, Region II) the behavior is consistent with that previously observed for $x = 0.33$, where CO within the CoO_2 layers stabilizes IC stripe-like SO with a cluster glass nature. For $x \gtrsim 0.6$ (Region III) the system remains paramagnetic down to low temperatures. We examine the data in each region in more detail below.

Region I. Data measured on the $x = 0$ compound La_2CoO_4 at SμS show oscillations in the asymmetry for $T \lesssim 75\,K$ [Fig. 2(c)], confirming a transition to SO. The asymmetry spectra within the ordered regime were found to be best fitted for $t \leqslant 0.5\,\mu s$ to the two-frequency relaxation function
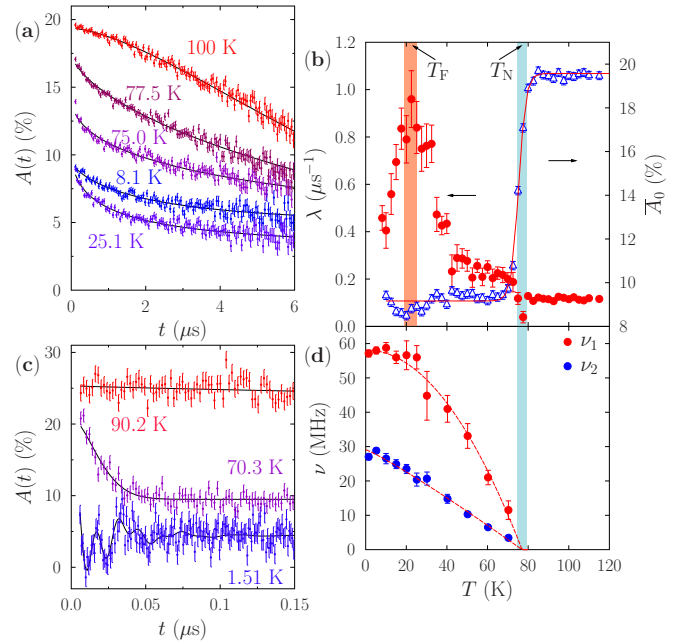

FIG. 2. Asymmetry data for $x = 0$ measured at (a) ISIS and (c) SμS showing spontaneous precession at low T (1.51 K data shifted by -5% for clarity). (b) Relaxation rate and early-time asymmetry $\overline{A}_0$, used to determine T_F and T_N, respectively. (d) Evolution of the two precession frequencies.

$A(t) = \sum_{i=1,2} A_i \cos(2\pi \nu_i t)e^{-\lambda_i t} + A_{\rm rel}e^{-\lambda_{\rm rel}t}$, where the oscillatory components, with amplitudes $A_{1,2}$ fixed to their average values, indicate two magnetically inequivalent muon stopping sites. The fitted values of the precession frequencies $\nu_{1,2}$ are plotted in Fig. 2(d), and drop to zero at a temperature $T_{\rm N}$, as expected for a magnetic transition to a paramagnetic state. Measurements made at ISIS are well suited to probing the slow dynamics of the system [Fig. 2(a)]. An abrupt drop in average early-time asymmetry is apparent upon cooling below $T \approx 75$ K [Fig. 2(b)] and a fit to the broadened step function yielded a value of $T_{\rm N} = 77(2)$ K, consistent with the vanishing of the oscillations. Upon further cooling below $T \approx 70$ K $\overline{A}_0$ does not change, but the longitudinal relaxation rate increases to a peak at around 22.5 K, before dropping again at lower temperatures. This is suggestive of a freezing of dynamics (as the correlation time τ increases) at lower temperatures than the transition to magnetic long-range SO. This feature is shared by the $x = 0.01$ sample, possibly indicating that the introduction of frustration by small concentrations of $S = 0$ Co^{3+} ions induces a freezing transition for a relaxation channel that has a characteristic time scale within the μSR dynamical range. The freezing is visible in the asymmetry spectra below $T_{\rm F}$ [see Fig. 2(a)] as an increase in the nonrelaxing baseline amplitude, reflecting those components of muon-spin polarization parallel to the local magnetic field, which can only be relaxed by dynamic field fluctuations.

We note that the value of $T_{\rm N}$ for $x = 0$ is considerably suppressed compared to the accepted value of 275 K reported in Ref. [23]. We attribute this to oxygen nonstoichiometry, which is an alternative route to doping holes into the CoO$_2$ layers (for La$_{2-x}$Sr$_x$CoO$_{4+\delta}$ the hole density is given by $n_{\rm h} = x + 2\delta$), as seen in the cuprate and nickelate systems [24,25]. Further annealing of an $x = 0$ sample led to a restored value of $T_{\rm N} \approx 275$ K; however, the lowered amplitude of the μSR signal and our subsequent NMR measurements indicate that the annealing process introduces impurity phases, particularly at the surfaces of the crystals. As Sr is introduced within region I ($x < 0.2$), $T_{\rm N}$ is found to drop abruptly to around 30 K by $x \approx 0.1$. This effect, together with that of the oxygen nonstoichiometry, demonstrates the sensitivity of the magnetism within the LSCO system to the concentration of nonmagnetic Co^{3+} ions within the CoO$_2$ layers. The presence of holes due to excess oxygen dramatically suppresses the onset temperature compared to the pristine compound, and $T_{\rm N}$ is further reduced rapidly by further addition of holes via Sr doping. This is in contrast to both the previously reported phase diagram [8], and the predictions of percolation theory for static nonmagnetic impurities in two dimensions (2D) where long-range AFM SO would persist up to $x \approx 0.41$ [26,27]. However, the effect is much less abrupt than in the superconducting series La$_{2-x}$Sr$_x$CuO$_4$, where long-range SO is replaced by an IC spin-glass phase by just $x = 0.02$ [28] (we find $\frac{dT_{\rm N}}{dx} \approx -10^3$ K/doped hole at low x; an order of magnitude smaller than in the cuprate series). The freezing temperature $T_{\rm F}$ does not decrease in the same manner, but remains at around 25 K across region I. The convergence of $T_{\rm N}$ and $T_{\rm F}$ above around $x = 0.1$ suggests that for these concentrations the peak in relaxation rate is sensitive to the critical divergence in correlation times accompanying the transition to magnetic SO on the muon time scale.

Region II. As more holes are introduced from further Sr substitution, a marked change in behavior for concentrations $x \geqslant 0.2$ is encountered, with samples in the region $0.2 \leqslant x \leqslant 0.5$ showing similar responses, suggestive that they share common features which might relate to stripe ordering. Stripe order in LSCO has been proposed for $x \geqslant 0.3$ on the basis of neutron scattering experiments [8]. Doping away from the parent compound introduces disorder and frustration into the planes and intermediate doping levels lead to short-range stripe correlations which stabilize IC magnetic order. The most robust CO is checkerboard CO, which occurs at $x = 0.5$ [29,30], where in-plane CO correlation lengths are largest [8]. Despite having different electronic properties to the cuprates, LSCO samples with $x = 0.33$ and 0.25, which exhibit disordered stripe CO correlations, display the distinctive hourglass magnetic excitation spectrum [31–37]. However, the origin of the hourglass spectrum and the nature of the CO in this region remain controversial [38–40]. The results of μSR and NMR measurements of the $x = 1/3$ compound revealed the onset of magnetic order within partially disordered charge and spin stripes at around 35 K, with a further glassy freezing of dynamics involving the slow, collective motion of spins within the magnetic stripes at lower temperatures [9]. We find that the μSR of $x = 0.25$ is similar to the $x = 0.33$ material, although the slightly broader features preclude the identification of a second freezing feature at lower temperatures.

A key observation is that the behavior of $x = 0.2$ is markedly different than samples in region I and suggests stripe correlations exist to lower concentrations x than previously believed. Asymmetry spectra obtained at SμS [Fig. 3(a)] show oscillations for temperatures below around 40 K, which were best fitted to the single-frequency relaxation function $A(t) = A_{\rm osc}\cos(2\pi\nu t + \varphi)e^{-\lambda_{\rm osc}t} + A_{\rm rel}e^{-(\Lambda t)^\beta} + A_{\rm b}$. Broad peaks in the temperature dependence of both longitudinal relaxation rate Λ and amplitude $A_{\rm rel}$ [Figs. 3(b) and 3(c)] suggest a freezing temperature $T_{\rm F} = 38(7)$ K. Upon cooling below 20 K, there is a gradual increase in the nonrelaxing contribution $A_{\rm b}$ [Figs. 3(a) and 3(b)], which points to a more static field distribution. Taken together, these results are consistent with slow dynamics within spatially inhomogeneous disordered stripes of magnetic Co^{2+} ions which start to freeze upon cooling for $T \lesssim 40$ K, with regions of static, glassy SO appearing as temperatures are lowered further. This description is consistent with a cluster glass, previously observed only at higher x [37].

The $x = 0.5$ compound has been of special interest as it has been found to support checkerboard CO below around $T_{\rm CO} \approx 800$ K [18,29,30]. Susceptibility and neutron scattering measurements reveal magnetic correlations appearing for $T \lesssim 60$ K [18,41] and a spin freezing transition at around 30 K dominated by 180° antiferromagnetic interactions between Co^{2+} ions across the nonmagnetic Co^{3+} sites [18]. Our muon data show a broad drop in $\overline{A}_0$ on cooling through around 30 K, coinciding with a peak in relaxation rate and the appearance of heavily damped oscillations indicating the onset of SO. No features are observed around 60 K, where moments are still fluctuating outside of the muon time scale. We note that the high level of disorder for $x = 0.5$, indicated by the heavily damped oscillations, is surprising given the high charge ordering temperature for this compound. However,
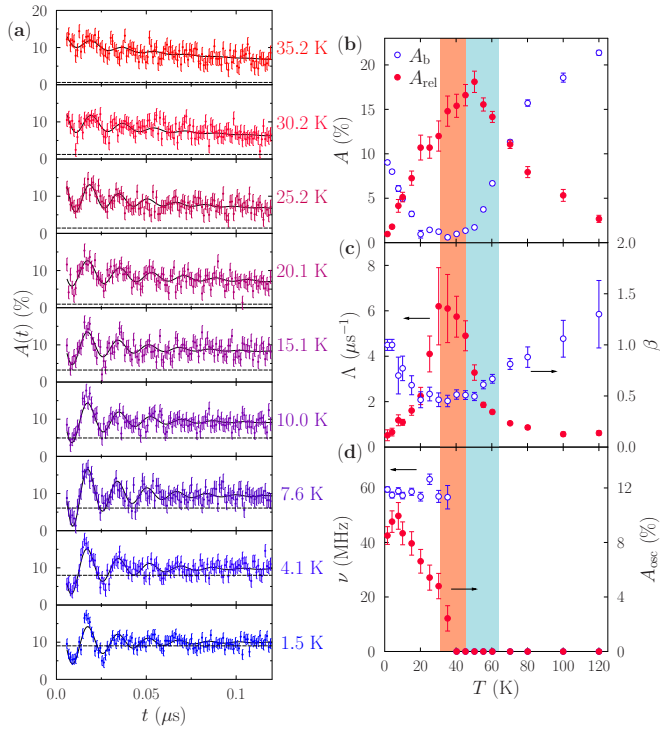
FIG. 3. (a) Asymmetry for $x = 0.2$ showing evolution of oscillations, and the nonrelaxing baseline (dashed horizontal lines). Solid lines are fits (see text). (b) Amplitude components; (c) longitudinal relaxation rate and exponent β; (d) amplitude and frequency of the oscillatory component.

the observation of a single oscillatory period provides a lower bound on the magnetic correlation length of around $10a \approx 4$ nm [42] (where a is the nearest-neighbor spin separation), which is consistent with previously reported in-plane correlation lengths [8,18,29].

Region III. For Sr concentrations $x \gtrsim 0.5$, neutron measurements have revealed short-range IC magnetic correlations on the neutron time scale [43], where glassy SO is likely to be accompanied by short-range CO. Our measurements in region III [10] detect no long-range SO on the muon time

scale down to the lowest measured temperatures (≈ 1.5 K) for the compounds $x = 0.67, 0.75$ and 0.9. For these samples, no muon precession is resolvable and full initial polarization is maintained at all temperatures. However, we see evidence of moments fluctuating more slowly as temperature is lowered below $T \approx 15$ K. If SO occurs above 1.5 K, then it could be short ranged or still fluctuating too rapidly on the muon time scale to be detectable.

In general, we note that for all temperatures of interest in this study ($T \leqslant 100$ K) the crystal structure of LSCO has been shown to be orthorhombic ($Bmab$ symmetry) for $x \leqslant 0.33$ and tetragonal ($I4/mmm$ symmetry) for $x \geqslant 0.4$ [8,39,40,44]. This structural transition does not coincide with either boundary of region II and so does not appear to be a driving factor for the magnetic behavior in this system.

The unique high- and low-spin nature of the magnetic and charge ordered cobalt ions in LSCO, and its insulating nature, means comparisons to other isostructural systems should be treated with caution. However, we note that our revised phase diagram does share some features with those of the cuprates and nickelates. The rapid suppression of T_N with increasing x in lightly doped samples is reminiscent of $La_{2-x}Sr_xCuO_4$ and other cuprates, where local probe measurements also reveal a continuous spin-freezing transition at temperatures well below that of magnetic ordering [45–48]. Our results indicate that the behavior associated with region II extends over a broad range of x, implying that the phase diagram bears a greater similarity to that of $La_{2-x}Sr_xNiO_4$ [6,49–52]. However, the stripe phase in the nickelate system is of a very different character, since the charge stripes themselves remain magnetically active [53].

[1] B. Keimer, S. A. Kivelson, M. R. Norman, S. Uchida, and J. Zaanen, Nature (London) **518**, 179 (2015).

[2] E. Fradkin and S. A. Kivelson, Nat. Phys. **8**, 864 (2012).

[3] J. M. Tranquada, Phys. B (Amsterdam, Neth.) **407**, 1771 (2012).

[4] J. M. Tranquada, B. J. Sternlieb, J. D. Axe, Y. Nakamura, and S. Uchida, Nature (London) **375**, 561 (1995).

[5] R. Comin and A. Damascelli, Annu. Rev. Condens. Matter Phys. **7**, 369 (2016).

[6] H. Ulbrich and M. Braden, Phys. C (Amsterdam, Neth.) **481**, 31 (2012).

[7] C. F. Chang, Z. Hu, H. Wu, T. Burnus, N. Hollmann, M. Benomar, T. Lorenz, A. Tanaka, H.-J. Lin, H. H. Hsieh, C. T. Chen, and L. H. Tjeng, Phys. Rev. Lett. **102**, 116401 (2009).

[8] M. Cwik, M. Benomar, T. Finger, Y. Sidis, D. Senff, M. Reuther, T. Lorenz, and M. Braden, Phys. Rev. Lett. **102**, 057201 (2009).

[9] T. Lancaster, S. R. Giblin, G. Allodi, S. Bordignon, M. Mazzani, R. De Renzi, P. G. Freeman, P. J. Baker, F. L. Pratt, P. Babkevich, S. J. Blundell, A. T. Boothroyd, J. S. Möller, and D. Prabhakaran, Phys. Rev. B **89**, 020405(R) (2014).

[10] See Supplemental Material at http://link.aps.org/supplemental/10.1103/PhysRevB.93.140406 for further details of sample synthesis, the experimental procedure and data analysis, including a plot of data and fitted parameters for compounds in region III ($x \gtrsim 0.6$) and results from μSR measurements made on the related compound $La_{2-x}Sr_xNiO_4$, for $x = 0.5$.

[11] A. Nemudry, P. Rudolf, and R. Schöllhorn, Solid State Ionics **109**, 213 (1998).

[12] F. Girgsdies and R. Schöllhorn, Solid State Commun. **91**, 111 (1994).

[13] L. Le Dreau, C. Prestipino, O. Hernandez, J. Schefer, G. Vaughan, S. Paofai, J. M. Perez-Mato, S. Hosoya, and W. Paulus, Inorg. Chem. **51**, 9789 (2012).

[14] D. Prabhakaran, P. Isla, and A. T. Boothroyd, J. Cryst. Growth **237-239**, 815 (2002); W.-J. Jang and H. Takei, Jpn. J. Appl. Phys. **30**, 251 (1991).

[15] S. J. Blundell, Contemp. Phys. **40**, 175 (1999).

[16] N. Hollmann, M. W. Haverkort, M. Cwik, M. Benomar, M. Reuther, A. Tanaka, and T. Lorenz, New J. Phys. **10**, 023018 (2008).

[17] N. Hollmann, M. W. Haverkort, M. Benomar, M. Cwik, M. Braden, and T. Lorenz, Phys. Rev. B **83**, 174435 (2011).

[18] L. M. Helme, A. T. Boothroyd, R. Coldea, D. Prabhakaran, C. D. Frost, D. A. Keen, L. P. Regnault, P. G. Freeman, M. Enderle, and J. Kulda, Phys. Rev. B **80**, 134414 (2009).

[19] For concentrations $x \geqslant 0.67$ no drop in initial asymmetry is observed in the data upon cooling. The early-time averaging was modified to use the time window $t \leqslant 0.015\,\mu$s, and normalized between 0 and the maximum value of $\overline{A}_0$.

[20] A. J. Steele, T. Lancaster, S. J. Blundell, P. J. Baker, F. L. Pratt, C. Baines, M. M. Conner, H. I. Southerland, J. L. Manson, and J. A. Schlueter, Phys. Rev. B **84**, 064412 (2011).

[21] For this analysis the early-time averaging criterion of $t \leqslant 0.015\,\mu$s was utilized for data measured at SμS, to take fuller advantage of the increased time resolution relative to ISIS data.

[22] R. S. Hayano, Y. J. Uemura, J. Imazato, N. Nishida, T. Yamazaki, and R. Kubo, Phys. Rev. B **20**, 850 (1979).

[23] K. Yamada, M. Matsuda, Y. Endoh, B. Keimer, R. J. Birgeneau, S. Onodera, J. Mizusaki, T. Matsuura, and G. Shirane, Phys. Rev. B **39**, 2336 (1989).

[24] B. O. Wells, Y. S. Lee, M. A. Kastner, R. J. Christianson, R. J. Birgeneau, K. Yamada, Y. Endoh, and G. Shirane, Science **277**, 1067 (1997).

[25] J. M. Tranquada, Y. Kong, J. E. Lorenzo, D. J. Buttrey, D. E. Rice, and V. Sachan, Phys. Rev. B **50**, 6340 (1994).

[26] M. E. J. Newman and R. M. Ziff, Phys. Rev. Lett. **85**, 4104 (2000).

[27] O. P. Vajk, P. K. Mang, M. Greven, P. M. Gehring, and J. W. Lynn, Science **295**, 1691 (2002).

[28] M. Matsuda, M. Fujita, K. Yamada, R. J. Birgeneau, Y. Endoh, and G. Shirane, Phys. Rev. B **65**, 134515 (2002).

[29] I. A. Zaliznyak, J. P. Hill, J. M. Tranquada, R. Erwin, and Y. Moritomo, Phys. Rev. Lett. **85**, 4353 (2000).

[30] I. A. Zaliznyak, J. M. Tranquada, R. Erwin, and Y. Moritomo, Phys. Rev. B **64**, 195117 (2001).

[31] J. M. Tranquada, H. Woo, T. G. Perring, H. Goka, G. D. Gu, G. Xu, M. Fujita, and K. Yamada, Nature (London) **429**, 534 (2004).

[32] S. M. Hayden, H. A. Mook, P. Dai, T. G. Perring, and F. Doğan, Nature (London) **429**, 531 (2004).

[33] V. Hinkov, P. Bourges, S. Pailhès, Y. Sidis, A. Ivanov, C. D. Frost, T. G. Perring, C. T. Lin, D. P. Chen, and B. Keimer, Nat. Phys. **3**, 780 (2007).

[34] O. J. Lipscombe, S. M. Hayden, B. Vignolle, D. F. McMorrow, and T. G. Perring, Phys. Rev. Lett. **99**, 067002 (2007).

[35] G. Xu, J. M. Tranquada, T. G. Perring, G. D. Gu, M. Fujita, and K. Yamada, Phys. Rev. B **76**, 014508 (2007).

[36] A. T. Boothroyd, P. Babkevich, D. Prabhakaran, and P. G. Freeman, Nature (London) **471**, 341 (2011).

[37] S. M. Gaw, E. C. Andrade, M. Vojta, C. D. Frost, D. T. Adroja, D. Prabhakaran, and A. T. Boothroyd, Phys. Rev. B **88**, 165121 (2013).

[38] A. T. Savici, I. A. Zaliznyak, G. D. Gu, and R. Erwin, Phys. Rev. B **75**, 184443 (2007).

[39] Y. Drees, D. Lamago, A. Piovano, and A. C. Komarek, Nat. Commun. **4**, 2449 (2013).

[40] Y. Drees, Z. W. Li, A. Ricci, M. Rotter, W. Schmidt, D. Lamago, O. Sobolev, U. Rütt, O. Gutowski, M. Sprung, A. Piovano, J. P. Castellan, and A. C. Komarek, Nat. Commun. **5**, 5731 (2014).

[41] Y. Moritomo, K. Higashi, K. Matsuda, and A. Nakamura, Phys. Rev. B **55**, R14725(R) (1997).

[42] A. Yaouanc and P. Dalmas de Réotier, *Muon Spin Rotation, Relaxation, and Resonance* (Oxford University Press, Oxford, UK, 2011).

[43] N. Sakiyama, I. A. Zaliznyak, S.-H. Lee, Y. Mitsui, and H. Yoshizawa, Phys. Rev. B **78**, 180406(R) (2008).

[44] M. Cwik, Ph.D. dissertation, Universität zu Köln, 2007, http://kups.ub.uni-koeln.de/2198/.

[45] F. C. Chou, F. Borsa, J. H. Cho, D. C. Johnston, A. Lascialfari, D. R. Torgeson, and J. Ziolo, Phys. Rev. Lett. **71**, 2323 (1993).

[46] F. Borsa, P. Carretta, J. H. Cho, F. C. Chou, Q. Hu, D. C. Johnston, A. Lascialfari, D. R. Torgeson, R. J. Gooding, N. M. Salem, and K. J. E. Vos, Phys. Rev. B **52**, 7334 (1995).

[47] S. Sanna, G. Allodi, G. Concas, A. D. Hillier, and R. De Renzi, Phys. Rev. Lett. **93**, 207001 (2004).

[48] S. Sanna, F. Coneri, A. Rigoldi, G. Concas, S. R. Giblin, and R. De Renzi, Phys. Rev. B **82**, 100503(R) (2010).

[49] V. Sachan, D. J. Buttrey, J. M. Tranquada, J. E. Lorenzo, and G. Shirane, Phys. Rev. B **51**, 12742 (1995).

[50] H. Yoshizawa, T. Kakeshita, R. Kajimoto, T. Tanabe, T. Katsufuji, and Y. Tokura, Phys. Rev. B **61**, R854(R) (2000).

[51] R. Kajimoto, K. Ishizaka, H. Yoshizawa, and Y. Tokura, Phys. Rev. B **67**, 014511 (2003).

[52] Th. Jestädt, K. H. Chow, S. J. Blundell, W. Hayes, F. L. Pratt, B. W. Lovett, M. A. Green, J. E. Millburn, and M. J. Rosseinsky, Phys. Rev. B **59**, 3775 (1999).

[53] A. T. Boothroyd, P. G. Freeman, D. Prabhakaran, A. Hiess, M. Enderle, J. Kulda, and F. Altorfer, Phys. Rev. Lett. **91**, 257201 (2003).